GEOLOGICA CARPATHICA, JUNE 2009, 60, 3, 193–204 doi: 10.2478/v10096-009-0013-4

Eclogites overprinted in the granulite facies from the Ďumbier Crystalline Complex (Low Tatra Mountains, Western Carpathians)

MARIAN JANÁK[1*], TOMÁŠ MIKUŠ[2], PAVEL PITOŇÁK[3] and JÁN SPIŠIAK[4]

[1]Geological Institute, Slovak Academy of Sciences, Dúbravská cesta 9, P.O. Box 106, 840 05 Bratislava 45, Slovak Republic;
*✉marian.janak@savba.sk
[2]Geological Institute, Slovak Academy of Sciences, Severná 5, 974 01, Banská Bystrica, Slovak Republic
[3]ENVIGEO, a.s., Kynceľová 2, 974 11 Banská Bystrica, Slovak Republic
[4]Faculty of Natural Sciences, Matej Bel University, Tajovského 40, 974 01 Banská Bystrica, Slovak Republic; spisiak@fpv.umb.sk

(Manuscript received June 17, 2008; accepted in revised form October 23, 2008)

Abstract: Metabasites with evidence for breakdown of former eclogites and recrystallization under granulite facies conditions occur in the Ďumbier Crystalline Complex of the Low Tatra Mountains, Central Western Carpathains. Textural relationships, phase equilibrium modelling and thermobarometry have been used to determine the *P-T* evolution of these rocks. Omphacite diagnostic for the eclogites facies stage is absent but its former presence is inferred from the symplectitic intergrowths of clinopyroxene + plagioclase. The re-equilibration in high-pressure granulite facies conditions is demonstrated by the assemblage garnet + clinopyroxene (< 10 % Jd) + plagioclase + quartz. The phase equilibrium modelling using THERIAK-DOMINO program and conventional geothermobarometry suggest the *P-T* conditions of 750–760 °C and 1.1–1.5 GPa for the high-pressure granulite stage. Orthopyroxene formed in the clinopyroxene + plagioclase symplectites and kelyphites and coronas around garnet at *P-T* conditions of ca. 0.7–1.0 GPa and 650–700 °C. *P-T* evolution of granulitized eclogites is interpreted as the result of two metamorphic events; early Variscan eclogite facies metamorphism was followed by granulite facies thermal overprint in the Carboniferous time. The second metamorphic event was crucial for breakdown of eclogites, these are only seldom preserved in the pre-Alpine basement of the Western Carpathians.

Key words: Western Carpathians, Low Tatra Mountains, geothermobarometry, phase equilibrium, modelling, granulites, eclogites.

Introduction

A common textural feature in eclogites resulting from re-equilibration at pressures below those of the eclogite facies, is the replacement of eclogite facies omphacite by symplectitic intergrowths of sodic plagioclase and clinopyroxene with lower Na and Al content than the initial clinopyroxene. In most cases, it is diopside with jadeite content below 20 %. The resulting mineral assemblage of garnet + clinopyroxene + plagioclase + quartz is the same as that found in high-pressure mafic granulites without evidence of an eclogite facies evolution. Orthopyroxene is commonly formed in pressure conditions lower than the peak recorded pressure (O'Brien 1997; O'Brien & Rötzler 2003).

Overprinted eclogites occur in several complexes of the Variscan basement of the Western Carpathians in Slovakia. In these rocks a high-pressure, eclogitic stage has been inferred from symplectites indicating the breakdown of primary omphacite (e.g. Hovorka & Méres 1990; Hovorka et al. 1992; Janák et al. 1996, 1997; Janák & Lupták 1997; Korikovsky & Hovorka 2001; Faryad et al. 2005). Eclogites with preserved omphacite are rare. They have been found in the eastern part of the Low Tatra Mountains (Janák et al. 2003, 2007), which belongs to the Veporic Unit of the Western Carpathians. Here, eclogites occur as lenses and boudins in the kyanite-bearing gneisses. Omphacite with the highest jadeite content (~40 mol %) occurs as inclusions in the garnet whereas omphacite with lower jadeite content is present in the matrix. Most of the clinopyroxene has jadeite content below 19 mol %, forming the symplectites with plagioclase, amphibole and quartz.

In this paper we describe the overprinted eclogites from the western part of the Low Tatra Mountains which belongs to the Tatric Unit of the Western Carpathians. The investigated rocks show the microtextures indicative for breakdown of former eclogites and recrystallization under granulite facies conditions with formation of orthopyroxene. The paper describes the mineralogical and petrological features, which constrain the *P-T* evolution, supported by pseudosection modelling and thermobarometry. Preservation of eclogites is discussed within the context of the Variscan tectonometamorphic evolution of the Western Carpathians.

Geological setting

The studied eclogites come from the Ďumbier Crystalline Complex of the Low Tatra Mountains (Fig. 1). The Ďumbier Crystalline Complex is composed of pre-Mesozoic granitoids, high-grade felsic rocks (orthogneisses, granulites, paragneisses), metabasites and metaultramafic rocks (Spišiak & Pitoňák 1990; Biely et al. 1992; Krist et al. 1992;

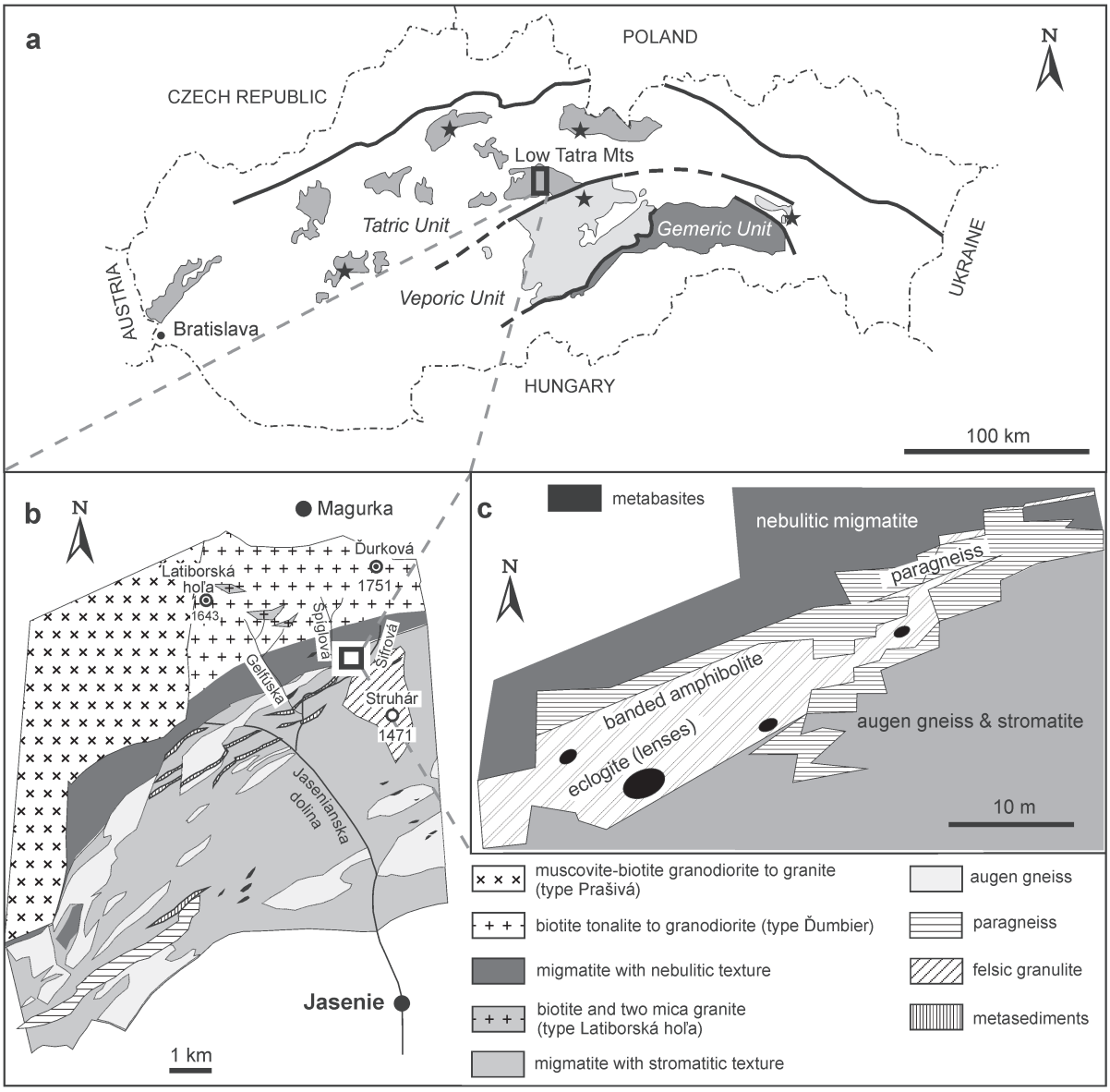

Fig. 1. Simplified geological maps of **a**) the Western Carpathians with occurrences of high-pressure metabasites (stars), **b**) the central part of the Ďumbier Crystalline Complex in the Low Tatra Mountains (modified from Biely et al. 1992), and **c**) the position of the investigated metabasites in the Jasenie-Kyslá ore deposit (according to Spišiak & Pitoňák 1990).

Petrík et al. 2006). The metamorphic rocks are intruded by a pluton which consists of several (Ďumbier, Prašivá and Latiborská hoľa) types of granitoid rocks, ranging from tonalite to granodiorite and granite. These magmatic rocks occur in the northern part of the area whereas metamorphic rocks form the southern belt with a transitional zone of migmatites at their contact (Bezák & Klinec 1983). The whole complex belongs to the upper tectonic unit (Putiš 1992; Janák 1994; Bezák et al. 1997; Plašienka et al. 1997) within the Variscan structure of the Western Carpathians.

Overprinted eclogites form dm–m lenses in banded amphibolites, also referred to as the "leptyno-amphibolite complex" (LAC) sensu Hovorka et al. (1994, 1997). Because of a lack of surface outcrops, most of such lenses were found underground, in the former mine for gold and tungsten, in the so called "Jasenie-Kyslá ore deposit" (Fig. 1). The whole complex is penetrated by veins of aplites and leucogranites. Metabasites are intimately associated with surrounding orthogneisses (augen-gneisses) and migmatites, all exhibiting mylonitization and shearing under ductile conditions. In the metapelitic gneisses sillimanite and very rarely kyanite partly transformed to sillimanite occur together with garnet, K-feldspar, plagioclase, biotite, muscovite, rutile and quartz. All the metamorphic rocks exhibit high-grade metamorphism and partial melting with formation of migmatites under granulite facies conditions, being partly retrogressed under amphibolite to greenschist facies conditions (Spišiak & Pitoňák 1990; Janák et al. 2000a,b; Mikuš et al. 2007). The crystalline basement is overlain by Mesozoic and Cenozoic sedimentary cover sequences and nappes.

The SHRIMP dating of zircon from banded amphibolites suggests an Ordovician (481±5 Ma) age for the magmatic protolith and two Variscan metamorphic events (428–411 and 338±6 Ma; Putiš et al. 2008). The electron microprobe dating of monazite from biotite gneisses and augen-gneisses gave mostly Carboniferous (350–340 Ma) ages, some monazite cores are older (ca. 470 and 390 Ma; Petrík et al. 2006). The age of the tonalite-granodiorite pluton (Ďumbier type) according to zircon dating (330±10, Poller et al. 2001; 343±3 Ma, Putiš et al. 2003) is Carboniferous.

Petrography

The investigated rocks come from the gallery no. 4 in the Šifrová dolina Valley north of Jasenie (Fig. 1). They exhibit a massive texture with reddish garnet and pale green clinopyroxene variably replaced by dark green amphibole. The sample J-257 comes from the core of a lens embedded in the leucocratic (trondhjemite-tonalite) and mafic (amphibolite, amphibole-biotite gneiss) layers (Fig. 2). This fabric is related to shearing and deformation during exhumation. The garnet and clinopyroxene-bearing lenses apparently represent relics of eclogites, preserved as boudins in the more retrogressed and deformed host rocks. The bulk rock composition of sample J-257 was determined by standard wet chemical analysis (Table 1).

Microstructures along with variations in mineral chemistry suggest that the investigated metabasites have experienced a complex metamorphic history. Four stages of recrystallization have been identified.

a) The *eclogite facies* stage is inferred from clinopyroxene + plagioclase symplectites after primary omphacite (Fig. 3a,c). Under the eclogites facies conditions the stable mineral assemblage may have consisted of garnet, omphacite, rutile and quartz with minor phengite and zoisite.

b) The *granulite facies* stage is demonstrated by replacement of omphacite by clinopyroxene + plagioclase symplectites and formation of orthopyroxene. The orthopyroxene occurs mostly in the kelyphitic rims and coronas together with plagioclase around garnet but also in the clinopyroxene + plagioclase symplectites (Fig. 3c,e); it is a later phase than garnet and clinopyroxene.

c) The *amphibolite facies* stage is manifested by formation of amphibole replacing pyroxenes and garnet; it is the most abundant phase of the matrix (Fig. 3e,f). Minor epidote, titanite, ilmenite, biotite and muscovite also belong to the amphibolite facies assemblage.

d) The *greenschist facies* stage is the latest one, with formation of actinolite, chlorite, quartz and calcite, mostly in the fractures and veins.

Fig. 2. Lens (boudin) of eclogite (sample J-257) embedded in the trondhjemite-amphibolite bands.

Mineral chemistry

The chemical composition of the major mineral phases was determined by CAMECA SX-100 electron microprobe at the State Geological Institute of Dionýz Štúr in Bratislava. The operating conditions were as follows: 15 kV accelerating voltage, 20 nA beam current, counting times 20 s on peaks and beam diameter of 2–10 μm. Mineral standards (Si, Ca: wollastonite, Na: albite, K: orthoclase, Fe: fayalite, Mn: rhodonite), pure element oxides (TiO_2, Al_2O_3, Cr_2O_3, MgO) and metals (Ni) were used for calibration. Raw counts were corrected using on-line PAP routine. Fe^{3+} in clinopyroxenes was calculated according to the charge balance proposed by Ryburn et al. (1976). Fe^{3+} in amphiboles was calculated assuming an ideal stoichiometry according to Schumacher (1997). The mineral abbreviations in this paper are according to Kretz (1983).

Garnet forms porphyroblasts with abundant inclusions in the cores (Fig. 3a,b). Some inclusions (amphibole, zoisite, rutile, phengitic white mica, quartz) may have been inherited from the prograde metamorphic stage but re-equilibrated in the high-pressure granulite stage as deduced from their composition. However, many "inclusions" (amphibole, plagioclase, epidote, chlorite, muscovite and quartz) are connected with matrix by fractures (Fig. 3a,b) and these were obviously related to fluids influx during the post-granulite retrogression. The garnets correspond to almandine (25–54 mol %) with significant grossular (22–27 mol %) and pyrope (19–30 mol %) contents (Table 2). The garnet compositional profile (Fig. 4) is relatively smooth, with an initial decrease of Prp and X_{Mg} concomitant with increase in X_{Fe} from the core to the rim at nearly constant Sps and slightly increasing Grs contents. A reverse pattern with slightly increasing Prp, X_{Mg} and de-

Table 1: Bulk rock composition of sample J-257 (wt. % oxides).

SiO_2	TiO_2	Al_2O_3	Fe_2O_3	FeO	MnO	MgO	CaO	Na_2O	K_2O	P_2O_5	H_2O	LOI	Total
48.86	1.03	14.04	1.75	7.72	0.18	10.61	8.86	1.91	1.52	0.1	0.31	3.1	99.99

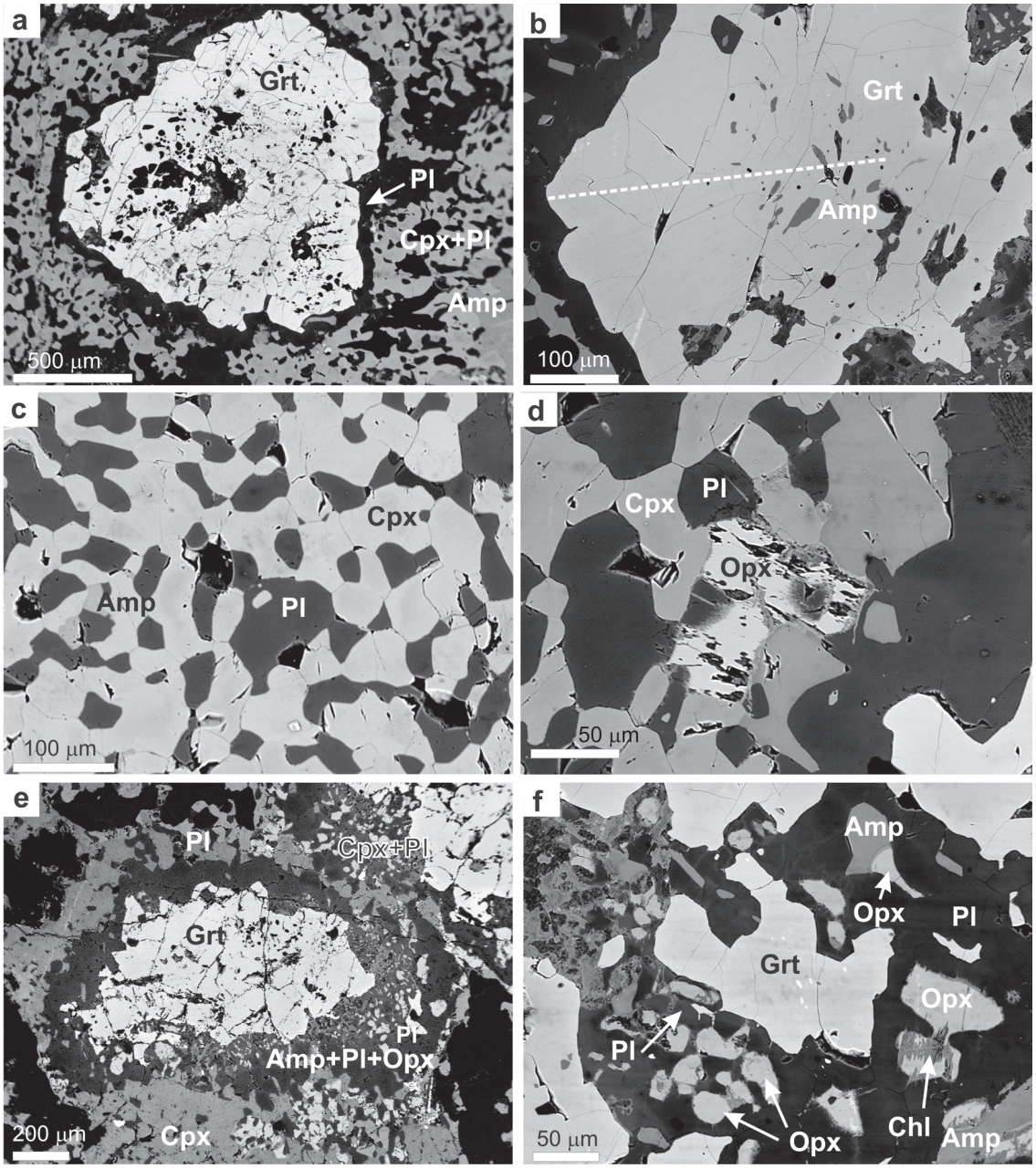

Fig. 3. Back-scattered electron (BSE) images. **a** — Garnet porphyroblast surrounded by plagioclase kelyphite. The matrix is composed of clinopyroxene + plagioclase symplectite and lath-shaped amphibole. **b** — Garnet porphyroblast with line marking the location of the analysed profile shown in Fig. 4. **c** — Symplectites of clinopyroxene + plagioclase partly replaced by amphibole. **d** — Symplectite of clinopyroxene + plagioclase partly replaced by orthopyroxene. Note a coarser clinopyroxene-plagioclase intergrowths. **e** — Garnet surrounded by orthopyroxene + plagioclase + amphibole kelyphite. **f** — Detail of orthopyroxene + plagioclase + kelyphite in corona around partly decomposed garnet. Orthopyroxene itself is partly replaced by chlorite.

creasing X_{Fe} can be observed in the medium part of garnet but close to the edge there is a decrease in Prp, X_{Mg} as well as Grs accompanied by increase in Sps, Alm and X_{Fe}. The maximum X_{Mg} occurs in the garnet cores whereas rims are depleted (Table 2). We infer that the actual rim of garnet that existed at the peak stage is no longer present. It has been consumed by the reactions producing kelyphite and corona textures. The observed zonation resulted from retrogression and partial resorption of garnet.

Clinopyroxene occurs as glomeroblastic and vermicular grains, symplectitically intergrown with plagioclase (Fig. 3). This indicates breakdown of primary, more Na and Al-rich clinopyroxene (omphacite) to secondary clinopyroxene and plagioclase. The characteristic "fingerprint" textures have mostly been recrystallized to coarser, granoblastic aggregates (e.g. Joanny et al. 1991; Anderson & Moecher 2007), where amphibole is also present (Fig. 3c). Symplectitic clinopyroxene is diopside (Table 3) with very low Al and Na contents (XJd≤0.1). It

Table 2: Representative microprobe analyses of garnet. Formula normalization to 12 oxygens.

anal. point	core	rim	core	rim	core	rim	core	rim
SiO_2	39.04	38.62	39.49	39.10	38.76	38.65	38.54	38.64
TiO_2	0.03	0.05	0.04	0.03	0.00	0.00	0.08	0.08
Al_2O_3	21.81	21.23	21.70	21.45	22.29	21.82	22.37	22.24
Cr_2O_3	0.02	0.30	0.01	0.07	0.00	0.00	0.00	0.00
FeO	24.30	25.93	24.23	24.25	21.52	22.77	22.33	23.21
MnO	0.87	1.18	0.82	1.03	0.80	0.85	0.74	1.01
MgO	5.53	4.74	6.37	5.27	7.60	5.67	6.24	5.56
CaO	9.26	9.06	8.16	9.79	8.53	9.87	9.55	9.90
Total	100.84	101.11	100.81	100.98	99.50	99.63	99.93	100.65
Si	3.001	2.989	3.012	3.026	2.980	2.999	2.971	2.974
Ti	0.002	0.003	0.002	0.003	0.000	0.000	0.005	0.005
Al	1.976	1.936	1.948	1.960	2.020	1.995	2.032	2.018
Cr	0.001	0.018	0.004	0.000	0.000	0.000	0.000	0.000
Fe^{3+}	0.087	0.097	0.093	0.085	0.085	0.085	0.082	0.086
Fe^{2+}	1.474	1.581	1.469	1.468	1.299	1.392	1.358	1.408
Mn	0.057	0.077	0.067	0.053	0.052	0.056	0.048	0.066
Mg	0.633	0.547	0.605	0.727	0.871	0.656	0.717	0.638
Ca	0.762	0.751	0.808	0.670	0.703	0.820	0.789	0.817
Total	8.009	8.002	8.010	7.991	8.010	8.003	8.014	8.013
X_{alm}	0.504	0.535	0.498	0.249	0.444	0.476	0.466	0.481
X_{sps}	0.019	0.026	0.023	0.503	0.018	0.019	0.017	0.022
X_{prp}	0.216	0.185	0.205	0.018	0.298	0.224	0.246	0.218
X_{grs}	0.249	0.240	0.261	0.220	0.231	0.269	0.260	0.267
X_{Mg}	0.300	0.257	0.292	0.331	0.401	0.320	0.346	0.312

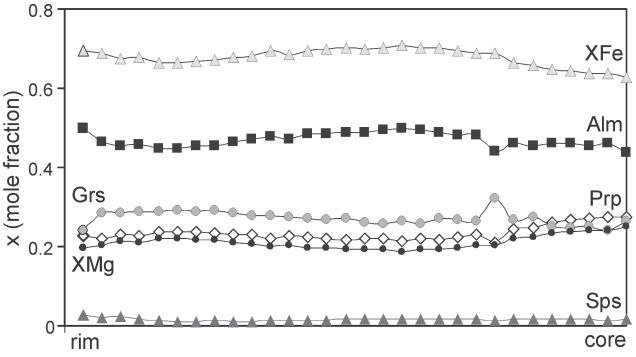

Fig. 4. Compositional profile across garnet shown in Fig. 3b. Length of profile is 400 μm.

shows slight compositional zoning with cores richer in Al and Na with respect to the rims (Table 3), which indicates recrystallization of more jadeitic clinopyroxene. Inclusions of clinopyroxene in garnet are small, their size is up to 10 μm and composition is similar to that of symplectitic clinopyroxene. The composition of the "primary" omphacite has been reconstructed from the modal proportions in clinopyroxene + plagioclase symplectites (BSE image at high magnification), converting the phase volumes (34 % Plg + 66 % Cpx) to weight % using densities of 2.7 $g \cdot cm^{-3}$ for plagioclase and 3.4 $g \cdot cm^{-3}$ for clinopyroxene. Average analysis of several symplectitic domains yields an initial jadeite content of 23 mol % (Table 3).

Orthopyroxene occurs in the clinopyroxene + plagioclase symplectitic domains (Fig. 3d) and in kelyphitic rims around garnets together with plagioclase and amphibole (Fig. 3e,f). The composition of orthopyroxene is almost uniform, with 0.26–0.28 X_{Mg} and < 0.5 wt. % CaO contents (Table 4).

Amphibole occurs as several compositional and textural types. Small euhedral crystals are enclosed in the garnet cores (Fig. 3b). In kelyphitic rims around garnets amphibole occurs as lath-shaped crystals, or vermicular intergrowths with orthopyroxene and plagioclase near the garnet (Fig. 3f). Matrix amphiboles are either large, strongly pleochroic, brown-green grains, or smaller grains that replace or form part of symplectites with clinopyroxene and plagioclase (Fig. 3c). These amphiboles are less aluminous and less sodic and correspond to Mg-hornblende (classification according to Leake 1997). Actinolite is a later phase, that formed zones around or grew along fractures within earlier amphiboles. Representative microprobe analyses of amphiboles are presented in Table 5.

Plagioclase textures suggest that it is a secondary phase formed due to the breakdown of garnet and clinopyroxene. Plagioclases in the symplectites with clinopyroxene have An_{25-30} (Table 6) whereas in the kelyphitic rims around garnets they have An_{48-78}. Albite occurs in domains containing chlorite and actinolite.

P-T evolution

The pressure and temperature conditions of metamorphism can be constrained using conventional mineral thermobarometers as well as pseudosection calculations (e.g. Powell & Holland 2008). Conventional thermobarometry employs the equilibrium thermodynamics of balanced reactions between minerals combined with the observed mineral end-member compositions. In contrast, pseudosections employ a method of Gibbs free energy minimization in a forward modelling of mineral parageneses for a given rock composition, with the potential to provide additional petrogenetic information. We used both methods to constrain the

Table 3: Representative microprobe analyses of clinopyroxene and recalculated composition of omphacite. Formula normalization to 6 oxygens and 4 cations.

type	in Grt	in Grt	symplect.	symplect.	symplect.	symplect.	symplect.	omp calc.
SiO_2	53.90	54.09	53.49	53.01	53.70	53.48	53.30	56.57
TiO_2	0.03	0.08	0.09	0.09	0.06	0.11	0.07	0.06
Al_2O_3	2.47	3.14	4.19	2.00	3.23	2.51	2.02	9.16
Cr_2O_3	0.10	0.08	0.08	0.09	0.01	0.14	0.12	0.00
FeO	5.87	6.88	6.43	8.12	6.49	8.34	6.60	4.98
MnO	0.19	0.13	0.13	0.12	0.17	0.14	0.07	0.09
MgO	14.19	14.16	13.48	14.12	13.65	13.92	14.69	10.10
CaO	22.13	21.56	21.12	22.31	21.80	22.27	22.06	16.97
Na_2O	1.05	1.28	1.41	0.44	1.08	0.67	0.80	3.43
K_2O	0.01	0.00	0.01	0.01	0.01	0.01	0.02	0.05
Total	99.94	101.40	100.42	100.30	100.20	101.60	99.79	101.41
Si	1.980	1.964	1.954	1.962	1.970	1.955	1.969	1.993
Ti	0.001	0.002	0.003	0.002	0.002	0.003	0.002	0.002
Al	0.107	0.134	0.180	0.087	0.140	0.108	0.088	0.381
Cr	0.003	0.002	0.002	0.003	0.000	0.004	0.003	0.000
Fe^{3+}	0.003	0.022	0.004	0.013	0.000	0.019	0.026	0.000
Fe^{2+}	0.178	0.187	0.193	0.239	0.199	0.236	0.178	0.147
Mn	0.006	0.004	0.004	0.004	0.005	0.004	0.002	0.003
Mg	0.777	0.767	0.734	0.779	0.747	0.759	0.809	0.531
Ca	0.871	0.839	0.827	0.885	0.857	0.872	0.873	0.641
Na	0.075	0.090	0.100	0.032	0.077	0.048	0.058	0.234
K	0.000	0.000	0.000	0.001	0.000	0.000	0.001	0.002
Total	4.001	4.011	4.002	4.006	3.997	4.009	4.010	3.933
X_{Jd}	0.07	0.06	0.09	0.01	0.07	0.02	0.03	0.23

Table 4: Representative microprobe analyses of orthopyroxene. Formula normalization to 6 oxygens and 4 cations.

SiO_2	52.50	52.69	51.98	52.38	52.78	52.56
TiO_2	0.04	0.05	0.05	0.06	0.03	0.05
Al_2O_3	0.95	0.72	0.70	0.40	0.61	0.74
Cr_2O_3	0.16	0.15	0.14	0.04	0.05	0.09
FeO	27.83	27.60	27.20	27.32	26.48	26.30
MnO	0.51	0.48	0.53	0.54	0.52	0.57
MgO	19.58	19.49	19.17	19.40	20.25	19.90
CaO	0.53	0.50	0.49	0.56	0.57	0.51
Na_2O	0.01	0.04	0.03	0.06	0.00	0.02
K_2O	0.01	0.02	0.01	0.01	0.00	0.01
Total	102.20	101.82	100.34	100.83	101.33	100.76
Si	1.961	1.972	1.975	1.980	1.977	1.979
Ti	0.001	0.001	0.002	0.002	0.001	0.001
Al	0.042	0.032	0.031	0.018	0.027	0.033
Cr	0.005	0.005	0.004	0.001	0.001	0.003
Fe^{3+}	0.030	0.021	0.013	0.018	0.017	0.006
Fe^{2+}	0.840	0.843	0.851	0.846	0.813	0.822
Mn	0.016	0.015	0.017	0.017	0.017	0.018
Mg	1.090	1.087	1.086	1.093	1.131	1.117
Ca	0.021	0.020	0.020	0.023	0.023	0.021
Na	0.001	0.003	0.002	0.004	0.000	0.001
K	0.001	0.001	0.001	0.001	0.000	0.001
Total	4.007	3.999	4.003	4.003	4.006	4.001
X_{Mg}	0.56	0.56	0.56	0.56	0.58	0.58

P-T evolution of the investigated metabasites from the Ďumbier Crystalline Complex.

The phase equilibrium modelling was performed with the THERIAK-DOMINO program (De Capitani 1994). This program performs a Gibbs free energy minimization using the algorithm of De Capitani & Brown (1987). For thermodynamic calculations, bulk rock composition of sample J-257 (Table 1) was used in the simplified system NCFMASH (Na_2O–CaO–FeO–MgO–Al_2O_3–SiO_2–H_2O), with water content in excess to model the water-saturated conditions (e.g. Carson et al. 1999; Guiraud et al. 2001). We assume that effective bulk composition (e.g. Stüwe 1997) was essentially homogeneous on the scale of measured sample. It was probably not significantly affected by the garnet fractionation process since there is an absence of growth zoning in the measured garnets but some parts of garnet that existed at the peak-pressure stage could have been removed from the equilibrating volume of rock by reactions consuming garnet and producing kelyphite and corona textures. We used the program DOMINO with the internally consistent mineral database (JUN92, an updated version of that of Berman 1988) and solid solution models for garnet (Berman 1990), omphacite, amphibole (Meyre et al. 1997), feldspar (Fuhrman & Lindsley 1988) and orthopyroxene as available from the THERIAK-DOMINO website: http://titan.minpet.unibas.ch/minpet/theriak/theruser.html. The calculated equilibrium phase diagram is shown in Fig. 5. The isopleths of mineral compositions were computed for a fixed bulk composition with the program DOMINO. The isopleths corresponding to measured mineral compositions for garnet, omphacite, orthopyroxene and plagioclase constrain the *P-T* conditions of equilibrium assemblages (Fig. 6).

Pressure and temperature conditions were also calculated by the application of several standard geothermometers and

Table 5: Representative microprobe analyses of amphibole. Formula normalization to 23 oxygens and 16 cations.

type	in Grt	in Grt	kelyphite	kelyphite	symplect.	symplect.	matrix	matrix	matrix	matrix
SiO_2	46.50	49.01	49.51	46.93	48.88	47.08	52.18	49.05	53.59	52.06
TiO_2	0.98	0.79	0.82	1.52	0.75	0.66	0.57	1.05	0.32	0.53
Al_2O_3	12.54	8.31	7.87	10.15	8.34	9.96	5.35	7.87	4.34	5.87
Cr_2O_3	0.08	0.38	0.60	0.54	0.23	0.16	0.13	0.16	0.08	0.13
FeO_t	10.23	10.84	11.51	12.64	10.77	11.75	10.16	11.01	9.94	10.18
MnO	0.10	0.07	0.14	0.16	0.17	0.05	0.10	0.20	0.12	0.17
MgO	14.36	14.82	15.12	13.36	15.44	14.35	16.98	15.36	17.11	16.44
CaO	12.15	11.58	11.90	11.28	11.71	11.56	11.74	11.89	12.14	12.01
Na_2O	1.73	1.27	1.18	1.75	1.33	1.62	0.77	1.25	0.41	0.72
K_2O	0.24	0.18	0.18	0.24	0.14	0.21	0.04	0.15	0.07	0.10
Total	99.06	97.38	98.89	98.72	97.76	97.40	98.02	97.99	98.12	98.21
Si	6.561	7.007	6.984	6.698	6.935	6.748	7.316	6.967	7.531	7.305
Ti	0.104	0.085	0.087	0.164	0.080	0.071	0.060	0.112	0.034	0.056
Al^{IV}	1.439	0.993	1.016	1.302	1.065	1.252	0.684	1.033	0.469	0.695
Al^{VI}	0.647	0.408	0.292	0.405	0.330	0.430	0.200	0.285	0.250	0.276
Cr	0.009	0.043	0.067	0.061	0.026	0.018	0.014	0.018	0.009	0.014
Fe^{3+}	0.384	0.439	0.526	0.529	0.597	0.623	0.551	0.514	0.241	0.468
Fe^{2+}	0.824	0.857	0.832	0.980	0.681	0.786	0.640	0.794	0.927	0.727
Mn	0.012	0.009	0.017	0.020	0.020	0.006	0.012	0.024	0.014	0.020
Mg	3.021	3.160	3.179	2.842	3.266	3.066	3.549	3.253	3.585	3.439
Ca	1.838	1.773	1.799	1.725	1.780	1.775	1.764	1.810	1.828	1.806
Na^{M4}	0.162	0.227	0.198	0.275	0.220	0.225	0.209	0.190	0.112	0.194
Na^{A}	0.310	0.126	0.124	0.210	0.146	0.225	0.000	0.154	0.000	0.002
K	0.044	0.033	0.032	0.044	0.025	0.038	0.007	0.027	0.013	0.018
Total	16.349	16.153	16.145	16.246	16.158	16.250	15.995	16.170	16.007	16.009

Table 6: Representative microprobe analyses of plagioclase. Formula normalization to 8 oxygens.

anal. point	kelyphite	symplect.	symplect.	symplect.	kelyphite	kelyphite	symplect.	kelyphite
SiO_2	56.64	62.76	61.11	60.97	58.36	48.11	61.20	51.01
Al_2O_3	28.01	24.17	24.62	24.48	26.18	32.57	24.87	31.63
FeO	0.32	0.22	0.08	0.26	0.39	0.45	0.16	0.22
CaO	10.13	5.54	5.63	5.93	8.07	15.75	6.37	14.20
Na_2O	5.96	8.77	8.38	8.53	7.01	2.39	7.90	3.46
K_2O	0.07	0.16	0.04	0.13	0.08	0.05	0.13	0.05
Total	101.12	101.64	99.89	100.34	100.11	99.34	100.67	100.57
Si	2.521	2.743	2.714	2.705	2.610	2.219	2.701	2.309
Al	1.469	1.245	1.289	1.280	1.380	1.770	1.294	1.687
Fe	0.012	0.008	0.003	0.010	0.015	0.017	0.006	0.008
Ca	0.483	0.260	0.268	0.282	0.386	0.778	0.301	0.689
Na	0.514	0.743	0.722	0.734	0.608	0.213	0.676	0.304
K	0.004	0.009	0.002	0.007	0.004	0.003	0.007	0.003
Total	5.003	5.007	4.998	5.018	5.002	5.000	4.986	5.000
Ab	51.34	73.44	72.76	71.72	60.87	21.45	68.67	30.52
An	48.25	25.66	27.01	27.56	38.7	78.27	30.57	69.19
Or	0.41	0.9	0.23	0.72	0.43	0.28	0.76	0.29

geobarometers, determined by the coexisting mineral assemblage. Temperatures were obtained from garnet-clinopyroxene (Powell 1985; Krogh Ravna 2000) and garnet-orthopyroxene (Harley 1984; Sen & Bhattacharya 1984) geothermometers. In garnet + clinopyroxene + plagioclase + quartz assemblages, pressures were calculated from the Mg end-member reaction according to Newton & Perkins (1982), Moecher et al. (1988) and Powell & Holland (1988). In Powell & Holland's calibration, both Hodges & Spear (1982), and Ganguly & Saxena (1984) garnet mixing models were employed. In those involving garnet + orthopyroxene + plagioclase + quartz, calibrations of Newton & Perkins (1982) and Powell & Holland (1988) with Mg end-member and Moecher et al. (1988) with Fe end-member reaction were used.

High-pressure granulite facies P-T conditions

As demonstrated above, the formation of clinopyroxene + plagioclase symplectites indicates a passage from eclogite facies to the high-pressure granulite facies (e.g. Zhao et al. 1991; O'Brien 1997; O'Brien & Rötzler 2003; Groppo et al. 2007). The *P-T* conditions of eclogite recrystallization and formation of high-pressure granulite facies assemblage garnet + clinopyroxene + plagioclase + amphibole + quartz have been modelled from the measured composition of garnet cores and clinopyroxene + plagioclase symplectites (Tables 2, 3 and 6). We used the garnet with the highest X_{Mg}, clinopyroxene with the highest jadeite, and plagioclase with the lowest anorthite in the calculations. The 0.4 X_{Mg} Grt,

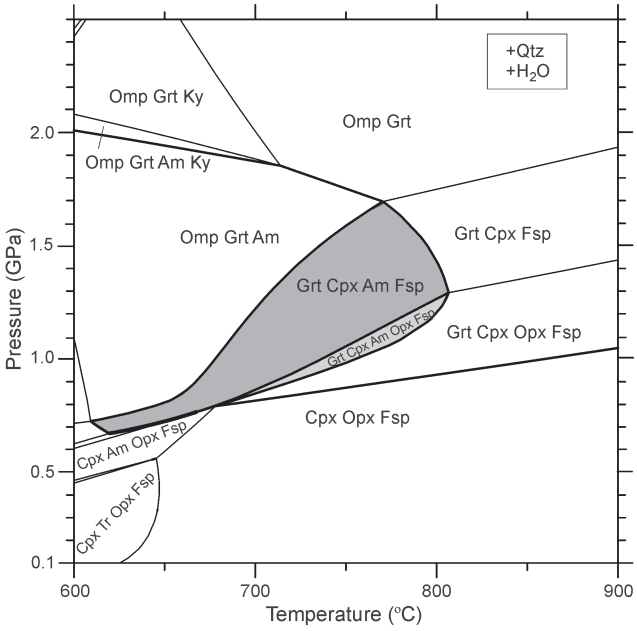

Fig. 5. Phase diagram for the composition of the investigated sample (J-257), calculated using the program DOMINO (De Capitani 1994). The shaded areas correspond to the observed assemblages. Quartz and H_2O are considered to be in excess.

0.9 X_{Jd} Cpx and 0.25 X_{An} Plg isopleths constrain ca. 750–760 °C and 1.1–1.4 GPa stability field (Fig. 6). The isopleths of "reconstructed" omphacite (0.23 X_{Jd}) and measured garnet core composition intersect at 1.5–1.6 GPa and 750 °C. The *P-T* conditions calculated from the Grt-Cpx thermometers and the Grt-Cpx-Pl-Qtz barometers are 700–760 °C and 1.1–1.4 GPa (Table 7, Fig. 7).

Orthopyroxene formation P-T conditions

The formation of orthopyroxene appears to be at the expense of clinopyroxene and garnet. We infer that orthopyroxene was in equilibrium with kelyphitic plagioclase and the outermost rim of garnet. The *P-T* conditions were calculated from the composition of orthopyroxene and adjacent garnet and plagioclase. The modelled isopleths with 0.56–0.58 X_{Mg}Opx, 0.26–0.32 X_{Mg} Grt and 0.4–0.7 X_{An} Plg (Fig. 6) constrain the orthopyroxene formation at ca. 0.7–0.9 GPa and 680–700 °C. The Grt-Opx thermometers in combination with the Grt-Opx-Pl-Qtz barometers yield *P-T* conditions of 650–740 °C and 0.7–1.1 GPa (Table 7, Fig. 7).

Discussion

Eclogite facies rocks in the crystalline basement of the Western Carpathians are rare. Eclogites with preserved omphacite from the eastern part of the Low Tatra Mts near Heľpa show the maximum pressure and temperature conditions of around 2.5 GPa and 700 °C. The metamorphic *P-T* path reflects nearly isothermal decompression during exhumation (Janák et al. 2007; Fig. 8). In contrast, eclogites from Jasenie show a very strong overprint at ca. 1.5–1.1 GPa. As in many eclogites overprinted in granulite facies (e.g. O'Brien et al. 1992; O'Brien & Vrána 1995; Guo et al. 2002) the orthopyroxene-producing stage has not allowed major diffusive resetting of zoned garnet but has led to differential decomposition of garnet rim (O'Brien & Vrána 1995). Actual garnet composition in equilibrium with plagioclase, symplectitic Cpx and later Opx is therefore very difficult to determine. For this reason the local equilibrium and effective bulk system for calculating the *P-T* conditions of post-peak stage need to be considered. In spite of these difficulties, the application of phase equilibrium modelling and conventional geothermobarometry as described above, yields essentially consistent results for the investigated metabasites from Jasenie.

The eclogitic mineral assemblages are preserved because reactions during decompression commonly consume the rocks's fluid and the system becomes water-undersaturated. Extensive retrogression may occur due to external fluids infiltration (Heinrich 1982; Carson et al. 1999; Guiraud et al. 2001). These circumstances may explain the breakdown of the eclogitic assemblage in the investigated rocks. Water-saturated conditions can be deduced from the presence of phengite, zoisite and amphibole. Pargasitic amphibole can be stable in high-pressure conditions as documented by phase equilibrium modelling (Fig. 5) and experimental data (e.g. Poli & Fumagalli 2003) but the majority of amphibole forming the symplectites, kelyphites and matrix clearly postdates the peak pressure conditions. This can be related to external fluids infiltration, most probably from the dehydrating country rocks like the metapelitic gneisses and migmatites.

Moreover, we assume that thermal overprint in high-pressure granulite facies conditions played an important role in the evolution of these rocks. There are two possibilities to

Table 7: Summary of P(GPa)–T(°C) estimates based on thermobarometric calculations.

	Grt-Cpx			**Grt-Cpx-Pl**				
Assemblage	**P ref**	**T *P***	**T *KR***	**T ref**	**P *NP***	**P *PH+HS***	**P *PH+GS***	**P *M* Mg**
Grt+Cpx+Pl+Qtz	1	751	716	700	1.15	1.1	1.29	1.25
	1.5	760	733	800	1.26	1.21	1.38	1.36
	Grt-Opx			**Grt-Opx-Pl**				
	P ref	**T *H***	**T *SB***	**T ref**	**P *NP***	**P *PH+HS***		**P *M* Fe**
Grt+Opx+Pl+Qtz	0.7	659	717	650	0.76	0.72		0.94
	1	674	735	750	0.81	0.76		1.1

P — Powell (1985), ***KR*** — Krogh Ravna (2000), ***PH*** — Powell & Holland (1988), ***HS*** — Hodges & Spear (1982), ***H*** — Harley (1984), ***GS*** — Ganguly & Saxena (1984), ***SB*** — Sen & Bhattacharya (1984), ***NP*** — Newton & Perkins (1982), ***M*** — Moecher et al. (1985).

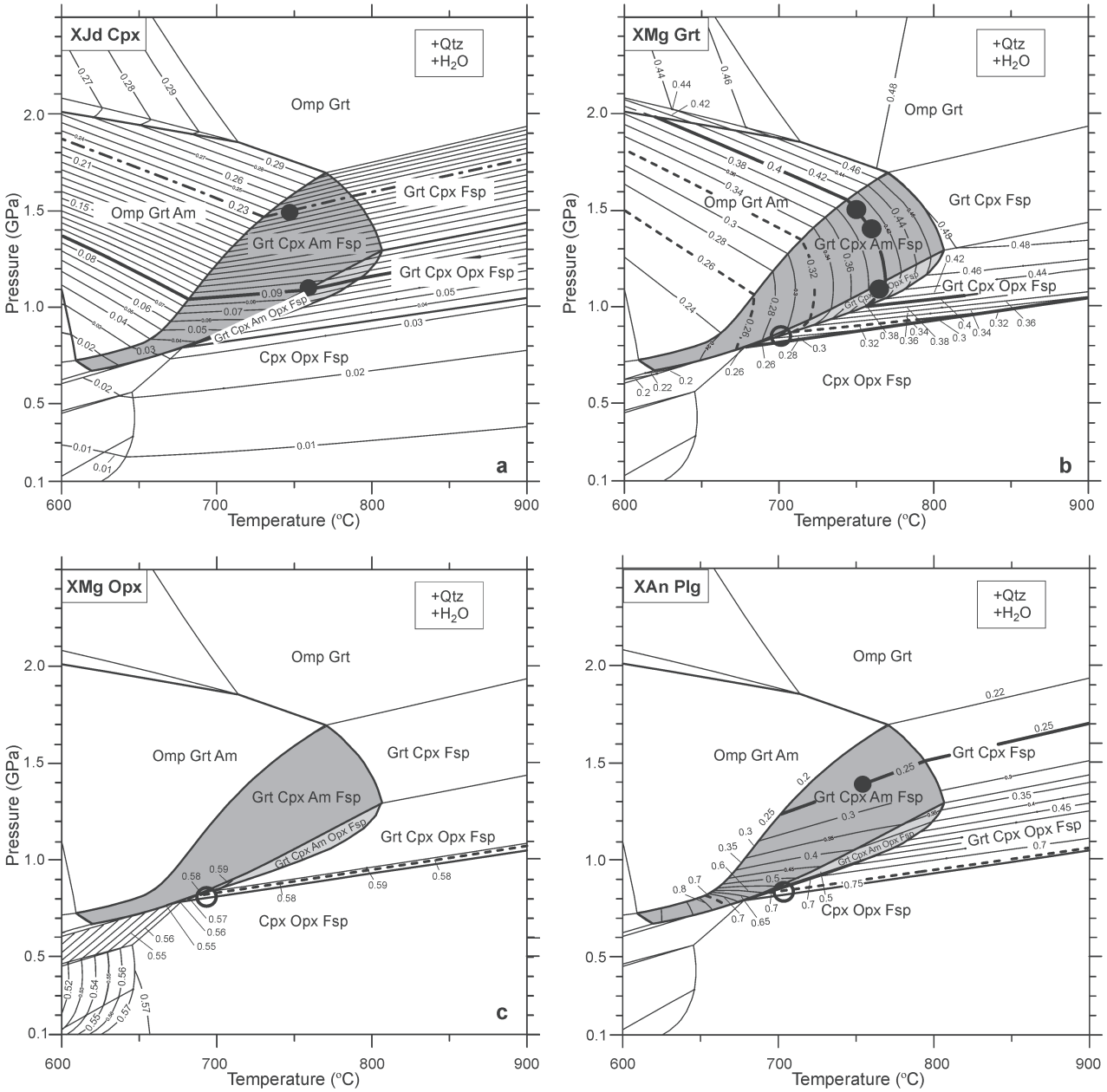

Fig. 6. Isopleths for **a** — X_{Jd} in clinopyroxene, **b** — X_{Mg} in garnet, **c** — X_{Mg} in orthopyroxene and **d** — X_{An} in plagioclase calculated with program DOMINO (De Capitani 1994). Bold lines refer to measured core compositions of garnet and symplectitic clinopyroxene and plagioclase. Dashed lines refer to measured compostions of garnet rims, orthopyroxene and kelyphitic plagioclase. Dashed-dotted line refers to reconstructed omphacite composition. The circles constrain the region of crosscutting of the isopleths. The bold circles mark the estimated peak *P-T* conditions and empty circles those of orthopyroxene formation.

explain such thermal overprint. Heating due to thermal relaxation and slow uplift during a single metamorphic event, or thermal overprint on partly exhumed eclogites due to a second metamorphic event.

Although the first alternative may be supported by texture with a relatively coarser clinopyroxene + plagioclase symplectites than that common in rapidly exhumed eclogites (Anderson & Moecher 2007), the second possibility is favoured from field relations and geochronological data. Overprinted eclogites with zircons of early Variscan age (Putiš et al. 2008) are accommodated in high-temperature and medium- to low-pressure rocks (mostly migmatites), some of them showing the transition of kyanite to sillimanite (Janák et al. 2000a). These are accompanied by voluminous granitoids of Carboniferous age (Petrík et al. 1994; Putiš et al. 2003; Petrík et al. 2006). Thermal overprint on partly exhumed eclogites seems to be related to metamorphism and partial melting at upper mantle/lower crustal levels. Following this overprint, the eclogites together with their host rocks were emplaced from the upper mantle/lower crustal depths by ductile extrusion and mid-crustal thrusting. In the Western Tatra, overprinted eclogites (Janák et al. 1996) and their

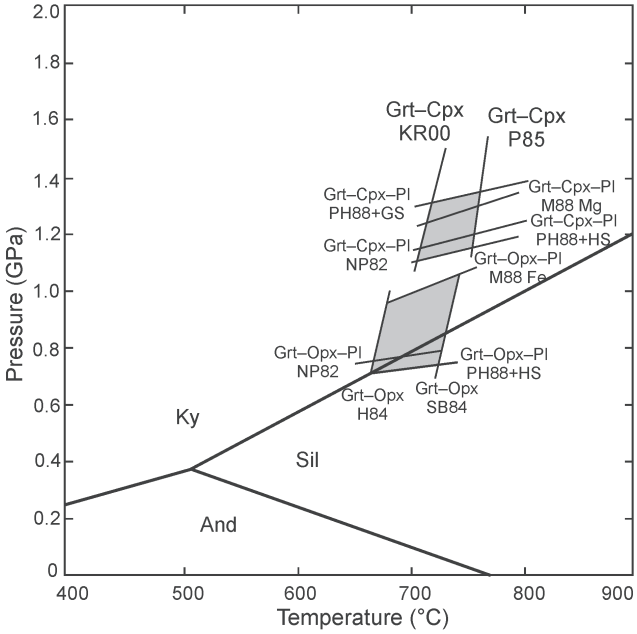

Fig. 7. Calculated *P-T* conditions from conventional geothermobarometry.

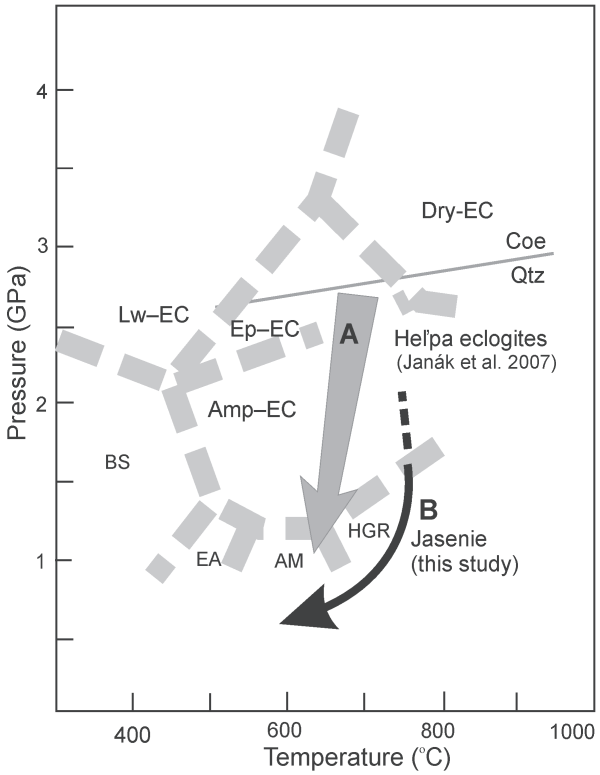

Fig. 8. *P-T* paths for eclogites from the Variscan basement of the Western Carpathians. **A** — eclogites from Heľpa (Janák et al. 2007), **B** — eclogites from Jasenie (this study). The metamorphic facies grid is from Okamoto & Maruyama (1999). **BS** — blueschist facies, **EA** — epidote amphibolite facies, **AM** — amphibolite facies, **HGR** — high-pressure granulite facies, **Lw–EC** — lawsonite eclogite facies, **Ep–EC** — epidote eclogite facies, **Amp–EC** — amphibole eclogite facies, **Dry–EC** — dry eclogite facies. The quartz-coesite curve is calculated from thermodynamic data of Holland & Powell (1998).

host rocks (Janák et al. 1999) are accommodated in a hangingwall (upper unit) of an inverted metamorphic sequence, above the micaschists.

There are similarities with granulitized eclogites from the internal parts of the Variscan orogen in the Bohemian Massif (e.g. O'Brien 2008). Here the eclogites formed earlier (420–380 Ma) than granulite-facies metamorphism (340 Ma), which was related to late stages of exhumation of the hot orogenic lower crust (Schulmann et al. 2002, 2008). We suggest that such thermal overprint during the Carboniferous time was crucial for the breakdown of eclogites in the Western Carpathians.

Conclusions

(1) Reaction textures and phase equilibrium modelling suggest that metabasites from the Ďumbier Crystalline Complex of the Western Carpathians underwent high-pressure metamorphism at eclogite facies conditions.

(2) The eclogites were re-equilibrated in high-pressure granulite facies conditions of 750–760 °C and 1.1–1.5 GPa. Orthopyroxene was formed in lower *P-T* conditions of ca. 0.7–1.0 GPa and 650–700 °C. Water-saturated conditions and thermal overprint facilitated the breakdown of eclogites during exhumation.

(3) Our study supports a two-stage tectonometamorphic evolution of the Western Carpathian's crystalline basement during the Variscan orogeny. The new data underline the close similarity with internal parts of the Variscan orogen in Central Europe.

Acknowledgments: We thank P. O'Brien, S.W. Faryad and I. Petrík for their helpful reviews. This work was supported by the Slovak Research and Development Agency under the contract APVV-51-046105, and Scientific Grant Agency VEGA, Grant No. 2/6092/26 and 2/0031/09. Thorsten Nagel (University of Bonn) is thanked for his help with the THERIAK-DOMINO program.

References

Anderson E.D. & Moecher D.P. 2000: Omphacite breakdown reactions and relation to eclogites exhumation rates. *Contr. Mineral. Petrology* 154, 242–252.

Berman R.G. 1988: Internally-consistent thermodynamic data for minerals in the system: Na_2O–K_2O–CaO–MgO–FeO–Fe_2O_3–Al_2O_3–SiO_2–TiO_2–H_2O–CO_2. *J. Petrology* 29, 445–522.

Berman R.G. 1990: Mixing properties of Ca–Mg–Fe–Mn garnets. *Amer. Mineralogist* 75, 328–344.

Bezák V. & Klinec A. 1983: The new interpretation of tectonic development of the Nízke Tatry Mts. — West part. *Geol. Zbor. Geol. Carpath.* 31, 569–575.

Bezák V., Jacko S., Janák M., Ledru P., Petrík I. & Vozárová A. 1997: Main Hercynian lithotectonic units of the Western Carpathians. In: Grecula P., Hovorka D. & Putiš M. (Eds.): Geological evolution of the Western Carpathians. *Miner. Slovaca–Monograph*, *Geocomplex*, Bratislava, 261–268.

Biely A., Beňuška P., Bezák V., Bujnovský A., Halouzka R., Ivanička J., Kohút M., Klinec A., Lukáčik E., Maglay J., Miko

O., Pulec M., Putiš M. & Vozár J. 1992: Geological map of the Nízke Tatry Mountains 1:50,000. *GÚDŠ*, Bratislava.

Carson C.J., Powell R. & Clarke G.L. 1999: Calculated mineral equilibria for eclogites in $CaO–Na_2O–FeO–MgO–Al_2O_3–SiO_2–H_2O$: application to the Pouébo Terrane, Pam Peninsula, New Caledonia. *J. Metamorph. Geology* 17, 9–24.

De Capitani C. 1994: "Gleichgewichts-Phasendiagramme" Theorie und Software. *Beihefte zum European Journal of Mineralogy, 72. Jahrestagung der Deutschen Mibneralogischen Gesellschaft*, 6, 48.

De Capitani C. & Brown T.H. 1987: The computation of chemical equilibrium in complex systems containing non-ideal solutions. *Geochim. Coscochim. Acta* 51, 2639–2652.

Faryad S.W., Ivan P. & Jacko S. 2005: Metamorphic petrology of metabasites from the Branisko and Čierna hora Mountains (Western Carpathians Slovakia). *Geol. Carpathica* 56, 3–16.

Fuhrman M.L. & Lindsley D.H. 1988: Ternary feldspar modeling and thermometry. *Amer. Mineralogist* 73, 201–215.

Ganguly J. & Saxena S.K. 1984: Mixing properties of aluminosilicate garnets: constraints from natural and experimental data and application to geothermo-barometry. *Amer. Mineralogist* 69, 88–97.

Groppo C., Lombardo B., Rolfo F. & Pertusati P. 2007: Clockwise exhumation path of granulitized eclogites from the Ama Drime range (Eastern Himalayas). *J. Metamorph. Geology* 25, 51–75.

Guiraud M., Powell R. & Rebay G. 2001: H_2O in metamorphism and unexpected behaviour in the preservation of metamorphic mineral assemblages. *J. Metamorph. Geology* 19, 445–454.

Guo J.H., O'Brien P.J. & Zhai M.G. 2002: High pressure granulites in the Sanggan area, North China craton: metamorphic evolution, P-T paths and geotectonic significance. *J. Metamorph. Geology* 20, 741–756.

Harley S. 1984: An experimental study of the partitioning of Fe and Mg between garnet and orthopyroxene. *Contr. Mineral. Petrology* 86, 359–373.

Heinrich C. 1982: Kyanite-eclogite to amphibolite facies evolution of hydrous mafic and pelitic rocks, Adula Nappe, Central Alps. *Contr. Mineral. Petrology* 81, 30–38.

Hodges K.V. & Spear F.S. 1982: Geothermometry, geobarometry and the Al_2SiO_3 triplepoint at Mt. Moosilauke, New Hampshire. *Amer. Mineralogist* 67, 88–97.

Holland T.J.B. & Powell R. 1998: An internally consistent thermodynamic data set for phases of petrological interest. *J. Metamorph. Geology* 16, 309–343.

Hovorka D. & Méres Š. 1990: Clinopyroxene-garnet metabasites from the Tribeč Mts. (Central Slovakia). *Miner. Slovaca* 22, 533–538.

Hovorka D., Méres Š. & Caňo F. 1992: Petrology of the garnet-clinopyroxene metabasites from the Malá Fatra Mts. *Miner. Slovaca* 24, 45–52.

Hovorka D., Méres Š. & Ivan P. 1994: Pre-Alpine Western Carpathians basement complexes: lithology and geodynamic setting. *Mitt. Österr. Geol. Gesell.* 86, 33–44.

Hovorka D., Méres Š. & Ivan P. 1997: Leptyno-amphibolite complex of the Western Carpathians: its definition, extent and genetical problems. In: Grecula P., Hovorka D. & Putiš M. (Eds.): Geological evolution of the Western Carpathians. *Miner. Slovaca–Monograph*, *Geocomplex*, Bratislava, 269–280.

Janák M. 1994: Variscan uplift of the crystalline basement, Tatra Mts., Central Western Carpathians: evidence from $^{40}Ar/^{39}Ar$ laser probe dating of biotite and P-T-t paths. *Geol. Carpathica* 45, 293–300.

Janák M. & Lupták B. 1997: Pressure-temperature conditions of high-grade metamorphism and migmatization in the Malá Fatra crystalline complex, the Western Carpathians. *Geol. Carpathica* 48, 287–302.

Janák M., O'Brien P.J., Hurai V. & Reutel C. 1996: Metamorphic evolution and fluid composition of garnet-clinopyroxene amphibolites from the Tatra Mountains, Western Carpathians. *Lithos* 39, 57–79.

Janák M., Hovorka D., Hurai V., Lupták B., Méres Š., Pitoňák P. & Spišiak J. 1997: High-pressure relics in the metabasites of the Western Carpathians pre-Alpine basement. In: Grecula P., Hovorka D. & Putiš M. (Eds.): Geological evolution of the Western Carpathians. *Miner. Slovaca–Monograph*, Bratislava, 301–308.

Janák M., Hurai V., Ludhová L., O'Brien P.J. & Horn E.E. 1999: Dehydration melting and devolatilization during exhumation of high-grade metapelites: the Tatra Mountains, Western Carpathians. *J. Metamorph. Geology* 17, 379–395.

Janák M., Chovan M., Smirnov A. & Majzlan J. 2000a: Kyanite and sillimanite in gneisses of Ďumbier crystalline complex, the Low Tatra Mountains. In: Uher P., Broska I., Jeleň S. & Janák M. (Eds.): Magurka 2000. *Geol. Inst. SAS*, Bratislava, 15.

Janák M., Pitoňák P. & Spišiak J. 2000b: Garnet-clinopyroxene metabasites from Jasenie, Low Tatra Mountains. In: Uher P., Broska I., Jeleň S. & Janák M. (Eds.): Magurka 2000. *Geol. Inst. SAS*, Bratislava, 14.

Janák M., Méres Š. & Ivan P. 2003: First evidence for omphacite and eclogite facies metamorphism in the Veporic unit of the Western Carpathians. *J. Czech Geol. Soc.* 48/1–2, 69–70.

Janák M., Méres Š. & Ivan P. 2007: Petrology and metamorphic P-T conditions of eclogites from the northern Veporic Unit (Western Carpathians, Slovakia). *Geol. Carpathica* 58, 121–131.

Joanny V., van Roermund H. & Lardeaux J.M. 1991: The clinopyroxene/plagioclase symplectite in retrograde eclogites: a potential geothermobarometer. *Geol. Rdsch.* 80, 303–320.

Korikovsky S.P. & Hovorka D. 2001: Two types of garnet-clinopyroxene-plagioclase metabasites in the Malá Fatra Mountains crystalline complex, Western Carpathians: Metamorphic evolution, P-T conditions, symplectitic and kelyphitic textures. *Petrology* 9, 119–141.

Kretz R. 1983: Symbols for rock forming minerals. *Amer. Mineralogist* 68, 277–279.

Krist E., Korikovsky S.P., Putiš M., Janák M. & Faryad S.W. 1992: Geology and petrology of metamorphic rocks of the Western Carpathian crystalline complexes. *Comenius University Press*, Bratislava, 1–324.

Krogh Ravna E.J.K. 2000: The garnet-clinopyroxene Fe^{2+}-Mg geothermometer: An updated calibration. *J. Metamorph. Geology* 18, 211–219.

Leake B.E. (Ed.), Woolley A.R., Arps C.E.S., Birch W.D., Gilbert M.C., Grice J.D., Hawthorne F.C., Kato A., Kisch J.H., Krivovichev V.G., Linthout K., Laird J., Mandarino J., Maresch W.V., Nickel E.H., Rock N.M.S., Schumacher J.C., Smith D.C., Stephenson N.C.N., Ungaretti L., Whittaker E.J.W. & Youzhi G. 1997: Nomenclature of amphiboles: Report of the Subcommittee on amphiboles of the International Mineralogical Association Commission on new minerals and mineral names. *Eur. J. Mineral.* 9, 623–651.

Meyre C., De Capitani C. & Partzsch J.H. 1997: A ternary solid solution model for omphacite and its application to geothermobarometry of eclogites from the Middle Adula nappe (Central Alps, Switzerland). *J. Metamorph. Geology* 15, 687–700.

Mikuš T., Janák M. & Spišiak J. 2007: Retrograded eclogites from the Ďumbier crystalline complex, Western Carpathians. CzechTec 07, 5th Meeting of the Central European Tectonic Studies Group (CETeG), April 11–14, 2007, Proceedings and excursion guide. *Czech Geol. Surv.*

Moecher D.P., Anovitz L.M. & Essene E.J. 1988: Calculation of clinopyroxene-garnet-plagioclase-quartz geobarometers and application to high grade metamorphic rocks. *Contr. Mineral. Petrology* 100, 92–106.

Newton R.C. & Perkins D. 1982: Thermodynamic calibration of geobarometers based on the assemblages garnet-plagioclase-othopyroxene (clinopyroxene)-quartz. *Amer. Mineralogist* 67, 203–222.

O'Brien P.J. 1997: Garnet zoning and reaction textures in overprinted eclogites, Bohemian Massif, European Variscides: a record of their thermal history during exhumation. *Lithos* 41, 119–133.

O'Brien P.J. 2008: Challenges in high-pressure granulite metamorphism in the aera of pseudosections: reaction textures, compositional zoning and tectonic interpretation with examples from the Bohemian Massif. *J. Metamorph. Geology* 26, 235–251.

O'Brien P.J. & Rötzler J. 2003: High-pressure granulites: formation, recovery of peak conditions and implications for tectonics. *J. Metamorph. Geology* 21, 3–20.

O'Brien P.J. & Vrána S. 1995: Eclogites with a short-lived granulite facies overprint in the Moldanubian Zone, Czech Republic: petrology, geochemistry and diffusion modeling of garnet zoning. *Geol. Rdsch.* 84, 473–488.

O'Brien P.J., Röhr C., Okrusch M. & Patzak M. 1992: Eclogite facies relics and a multistage breakdown in metabasites of the KTB pilot hole, NE Bavaria: implications for the Variscan tectonometamorphic evolution of the NW Bohemian Massif. *Contr. Mineral. Petrology* 112, 261–278.

Okamoto K. & Maruyama S. 1999: The high-pressure synthesis of lawsonite in the MORB + H_2O system. *Amer. Mineralogist* 84, 362–373.

Petrík I., Broska I. & Uher P. 1994: Evolution of the Western Carpathian granite magmatism: age, source rock, geotectonic setting and relations to the Variscan structure. *Geol. Carpathica* 45, 283–291.

Petrík I., Konečný P., Kováčik M. & Holický I. 2006: Electron microprobe dating of monazite from the Nízke Tatry Mountains orthogneisses (Western Carpathians, Slovakia). *Geol. Carpathica* 57, 4, 227–242.

Plašienka D., Grecula P., Putiš M., Hovorka D. & Kováč M. 1997: Evolution and structure of the Western Carpathians: an overview. In: Grecula P., Hovorka D. & Putiš M. (Eds.): Geological evolution of the Western Carpathians. *Miner. Slovaca–Monograph*, *Geocomplex*, Bratislava, 1–24.

Poli S. & Fumagalli P. 2003: Mineral assemblages in ultrahigh pressure metamorphism: A review of experimentally determined phase diagrams. *EMU notes in Mineralogy* 5, 10, 307–340.

Poller U., Janák M., Kohút M. & Todt W. 2000: Early Variscan magmatism in the Western Carpathians: U-Pb zircon data from granitoids and orthogneisses of the Tatra Mountains (Slovakia). *Int. J. Earth Sci.* 89, 336–349.

Poller U., Todt W., Kohút M. & Janák M. 2001: Nd, Sr, Pb isotope study of the Western Carpathians: implications for Palaeozoic evolution. *Schweiz. Mineral. Petrogr. Mitt.* 81, 159–174.

Powell R. 1985: Regression diagnostics and robust regression in geothermometer/geobarometer calibration: the garnet-clinopyroxene geothermometer revisited. *J. Metamorph. Geology* 3, 327–342.

Powell R. & Holland T.H.B. 1988: An internally consistent thermodynamic dataset with uncertainties and correlations: 3. Applications to geobarometry, worked examples and a computer program. *J. Metamorph. Geology* 6, 173–204.

Powell R. & Holland T.J.B. 2008: On thermobarometry. *J. Metamorph. Geology* 26, 155–179.

Putiš M. 1992: Variscan and Alpidic nappe structures of the Western Carpathians crystalline basement. *Geol. Carpathica* 43, 369–382.

Putiš M., Kotov A.B., Petrík I., Korikovsky S.P., Madarás J., Salnikova E.B., Yakovleva S.Z., Berezhnaya N.G., Plotkina Y.V., Kovach V.P., Lupták B. & Majdán M. 2003: Early- vs. Late orogenic granitoids relationships in the Variscan basement of the Western Carpathians. *Geol. Carpathica* 54, 163–174.

Putiš M., Sergeev S., Ondrejka M., Larionov A., Siman P., Spišiak J., Uher P. & Paderin I. 2008: Cambrian-Ordovician metaigneous rocks associated with Cadomian fragments in the West-Carpathian basement dated by SHRIMP on zircons: a record from the Gondwana active margin setting. *Geol. Carpathica* 59, 3–18.

Ryburn R.J., Raheim A. & Green D.H. 1976: Determination of P, T paths of natural eclogites during metamorphism — record of subduction. A correction to a paper by Rahaim and Green (1975). *Lithos* 9, 161–164.

Schulmann K., Schaltegger U., Ježek J., Thompson A.B. & Edel J.B. 2002: Rapid burial and exhumation during orogeny: thickening and syncorvengent exhumation of thermally weakened and thinned crust (Variscan orogen in Western Europe). *Amer. J. Sci.* 302, 856–879.

Schulmann K., Lexa O., Štípská P., Racek M., Tajčmanová L., Konopásek J., Edel J.B., Peschler A. & Lehmann J. 2008: Vertical extrusion and horizontal spreading of orogenic lower crust: a key exhumation mechanism in large hot orogens? *J. Metamorph. Geology* 26, 273–297.

Schumacher J.C. 1997: The estimation of the proportion of ferric iron in electron-microprobe analysis of amphiboles. *Canad. Mineralogist* 35, 238–246.

Sen S.K. & Bhattacharya A. 1984: An orthopyroxene-garnet thermometer and its application to the Madras charnokites. *Contr. Mineral. Petrology* 88, 64–71.

Spišiak J. & Pitoňák P. 1990: Nízke Tatry Mts. crystalline complex — new facts and interpretation (Western Carpathians, Czechoslovakia). *Geol. Zbor. Geol. Carpath.* 41, 377–392.

Stüwe K. 1997: Effective bulk composition changes due to cooling: a model predicting complexities in retrograde reaction textures. *Contr. Mineral. Petrology* 129, 43–52.

Zhao G., Cawood P.A., Wilde S.A. & Lu L. 2001: High-pressure granulites (retrograded eclogites) from the Hengshan Complex, North China craton: petrology and tectonic implications. *J. Petrology* 42, 1141–1170.